Proceedings of ITC18,2008

Toroidal flow velocity profile of an impurity ion in a Field-Reversed Configuration plasma

Tatsuya Ikeda, Toshiki Takahashi, Tomohiko Asai[a], Tsutomu Takahashi[a]

Department of Electronic Engineering, Gunma University, kiryu 376-8515, Japan

[a]College of Science and Technology, Nihon University, Tokyo 101-8308, Japan

Particle orbits of impurity ions are calculated to estimate their toroidal flow velocity. If the impurity ion flow differs from the ion flow, the Doppler shift measurement of impurity spectra requires a suitable modification of experimental results. At the field-null, the carbon ion flow coincides with the deuterium ion flow due to the friction force between them. At the separatrix, however, impurity and plasma ions have their own flow velocities. It is found that the diamagnetic drift that is dependent on the charge and mass of each fluid species dominates the toroidal flow velocity.

Keywords: field-reversed configuration, toroidal flow velocity, Doppler shift measurement, orbit calculation, resistive flux decay

1. Introduction

The rotational instability with the toroidal mode number n=2 limits the lifetime of field-reversed configuration (FRC) plasmas [1, 2]. Several works showed application of external multipole fields suppresses time variation of the line-integrated electron density [3, 4]. These experiments reveal elliptical deformation of FRC plasmas is inhibited by multipole fields. Internal structure, on the other hand, can be deformed to a complex dumbbell-like shape [5], even when no deformation of the separatrix shape can be found. Therefore, we need to clarify the origin of rotation to prolong the FRC lifetime.

Particle loss [6] and end-shorting [7] are now considered as two most promising mechanisms. Recently, Belova *et al*. claimed that particle loss associated with resistive flux decay may contribute to the rotation [8]. We have shown that the flux decay can contribute directly to the toroidal spin-up [9]. Suppose the FRC plasma is axisymmetric. This assumption is valid until the rotational instability is triggered. In this case, the canonical angular momentum

$$P_\theta = mv_\theta r + q\psi(r,z) \qquad (1)$$

of every particle is conserved, where m, q are the mass and charge, v_θ is the toroidal velocity component, and $\psi(r,z)$ is the poloidal flux function. If the poloidal flux decays due to a resistivity and toroidal axisymmetry is still valid, then

$$m\Delta(v_\theta r) = -q\Delta\psi \ . \qquad (2)$$

Equation (2) shows every ion gains the angular momentum in the ion diamagnetic direction, when the trapped poloidal flux decays. Generally, the separatrix radius decreases during the decay phase. If the guiding center r is also decreased, the toroidal velocity v_θ is further increased. The toroidal velocity for ions is calculated by averaging v_θ .

The toroidal velocity measurement is important to find its time evolution and spatial profile. Conventional method to find flow velocities is the Doppler shift measurement of impurity ion spectra such as C III and C V. If impurity ions rotate with the same velocity as plasma ions, then the Doppler shift measurement offers accurate information of plasma flow. Otherwise we need modification of the experimental result to obtain the rotation velocity.

In the present paper, we study numerically the impurity ion (carbon ion) velocity in an FRC plasma that decays resistively and therefore rotates according to Ref. 9.

2. Numerical Model

Since the discussion above is based on a single-particle picture, we need to confirm a collective effect due to the flux decay. A number of super-particles are traced numerically in the decaying FRC plasma. The poloidal flux decay is reproduced by

$$\frac{\partial\psi}{\partial t} = -r\eta J_\theta \ . \qquad (3)$$

Here, the electric resistivity η equals $A\eta_{\mathrm{cl}}$, where A is the anomaly factor and η_{cl} is the classical resistivity. Note that $\psi > 0$ inside the separatrix region in our paper. The flux lifetime is controlled by the parameter A . By integrating Eq. (3) with use of the Runge-Kutta method, a flux function at a calculation point is found. The

author's e-mail: m08e602@gs.eng.gunma-u.ac.jp

electromagnetic fields are then written by the obtained ψ as

$$\mathbf{B} = \nabla \times \mathbf{A} = \nabla \times \left(\frac{\psi}{r} \mathbf{e}_\theta \right), \quad \mathbf{J} = \frac{1}{\mu_0} \nabla \times \mathbf{B}, \quad \mathbf{E} = \eta \mathbf{J} \,. (4)$$

The plasma and impurity ions (C^{4+}) are traced as super-particles in the field given by Eq. (4). The weight of a super-particle is estimated initially from the Maxwell distribution. The friction term due to collisions is included in the equation of motion. The Pitch angle scattering is simulated with use of a Monte-Carlo method [10]. The density and particle flux of both plasma and impurity ions are calculated by the PIC method [11].

3. Results and Discussion

The orbit of an impurity ion is calculated in a prescribed field given in Eqs. (3) and (4). To compare our results with an FRC experiment, the flux decay time obtained by our calculation is set to be equal to the flux lifetime of the NUCTE (Nihon University Compact Torus Experiment)-III device. As noted before, the flux decay time is controlled by the anomaly factor A.

The time evolution of the trapped flux in the NUCTE-Ⅲ experiment is shown in Fig. 1. The FRC plasma is formed in 0-10 μs. The rotational instability with the toroidal mode number n=2 is caused at 35 μs, and the magnetic configuration collapses. From the end of the formation phase (t=10μs in Fig. 1), therefore the FRC plasma keeps axisymmetry for 25μs; it corresponds to $23t_{A0}$, where t_{A0} is the Alfvén time $t_{A0} \equiv r_w / v_{A0}$, and $v_{A0} \equiv B_{ex} / \sqrt{\mu_0 m_i n_0}$ (B_{ex} : the initial external magnetic field, m_i : the plasma ion mass, n_0 : the initial density at the field-null). The decrement of the trapped flux for $23t_{A0}$ is about 0.26 mWb. By controlling the anomaly factor, we obtain the time evolution of the flux shown in Fig. 2, where the decrement of the flux for $23t_{A0}$ is almost the same as the experimental result.

According to Ref. [9], presence of the resistive flux decay cause rotation of the FRC plasma. The calculated plasma ion density and toroidal velocity profile are shown by the color contour in Figs. 3 and 4. We can see that the plasma ions diffuse out from the separatrix by collisions. As the magnetic flux decays, ions can gain the toroidal momentum near the separatrix. This rotation velocity results from particle loss and the direct effect of flux decay.

The profiles of impurity ion density and flow velocity obtained by our calculation are presented in Figs. 5 and 6. The initial impurity density is set as $10^{-5} n_i$, where n_i is the ion density. We assume the impurity ion temperature is same as the plasma ion temperature, since collisions for thermal equilibrium are frequent in the formation phase.

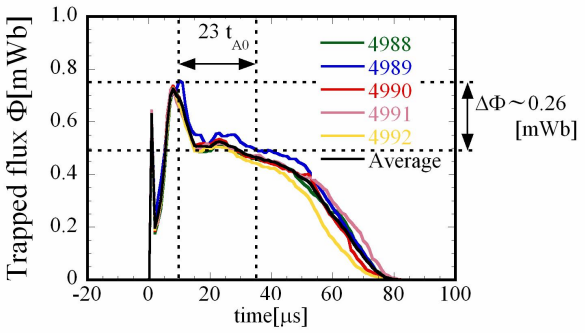

Fig.1 The time evolution of the trapped flux in the experiment that is used NUCTE-Ⅲ.

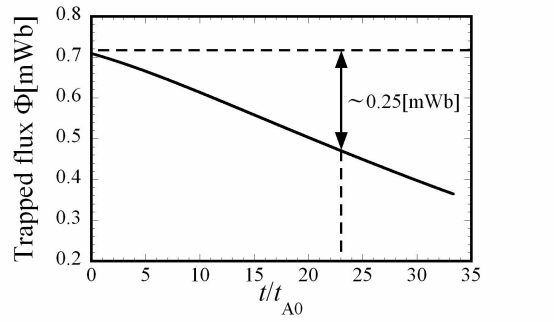

Fig.2 The time evolution of the maximum trapped flux obtained by the numerical calculation.

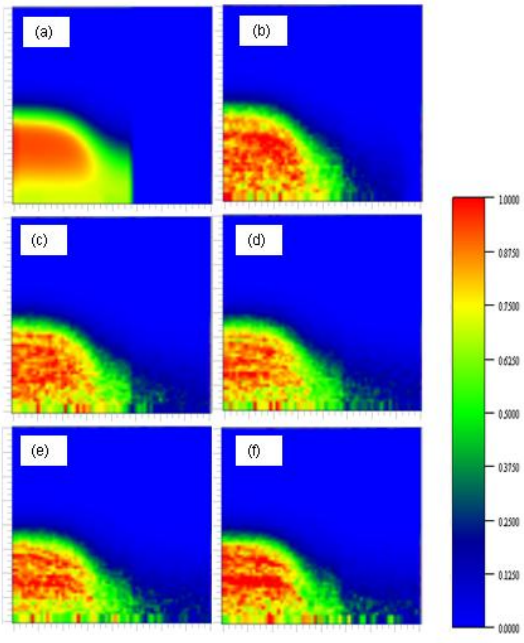

Fig.3 Color contours of the plasma ion density whose values are normalized by the initial density at the field-null. The figures are shown at (a) $t = 0$, (b) $t = 2t_{A0}$, (c) $t = 4t_{A0}$, (d) $t = 6t_{A0}$, (e) $t = 8t_{A0}$, and (f) $t = 10t_{A0}$.

The temperatures of both ions and impurity ions are 124 eV here. It is found that the impurity ions concentrate gradually at the field-null due to the $\mathbf{E}\times\mathbf{B}$ drift. The difference seen in the density profile between plasma and impurity ions results from their collision frequency. We also found the impurity ion density at the separatrix reduced significantly; it cause reduction in the diamagnetic drift velocity of impurity ions. From Fig. 6, we find the toroidal velocity peaks at the field-null point. At the separatrix, on the other hand, the rotation velocity vanishes after $t = 6t_{A0}$. The time evolution of toroidal velocity at the field-null is presented in Fig. 7. Significant time variation of ion velocity is caused by shortage of the number of super-particles. Also, averaged Larmor radius of deuterium ions is larger than the radial mesh interval. To reduce the amplitude of the oscillation, we need more super-particles as deuterium ions. It appears from Fig. 7 that the toroidal velocity of impurity ions follows the time averaged (coarse-grained in time) ion velocity. We can say that the Doppler shift measurement of impurity ion spectra is valid at the field-null point. Contrary to Fig. 7, the separatrix velocity of impurity ions deviates considerably as shown in Fig. 8. Although the ion density gradient is sustained, the impurity ions near the separatrix distributes uniformly. Therefore, the diamagnetic drift velocity reduces for the impurity ions. At the field-null point, the friction force acting on the impurity ion dominates the toroidal velocity, and then the velocity

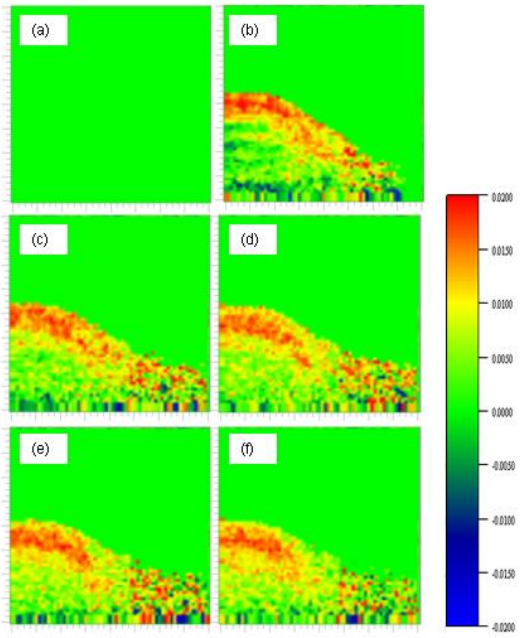

Fig.4 Color contours of the toroidal flow velocity for plasma ions. The velocity is normalized by r_w/τ, where $\tau \equiv m_i r_w^2/(q_i|\psi_w|)$. The output time is the same as Fig. 3.

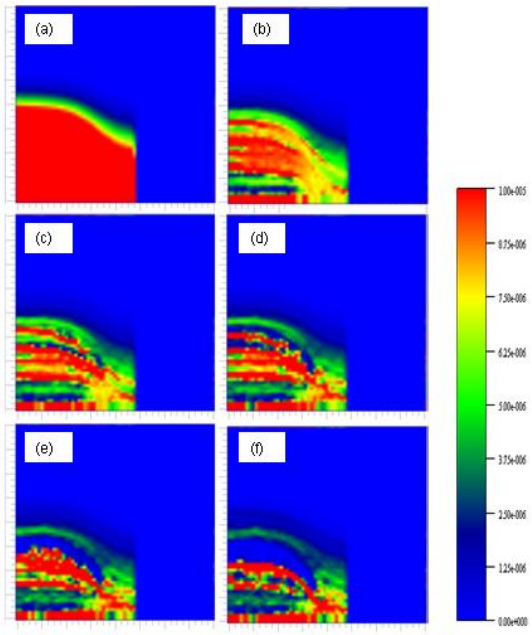

Fig.5 Color contours of the impurity ion density. Figures are shown in the same manner as Fig.

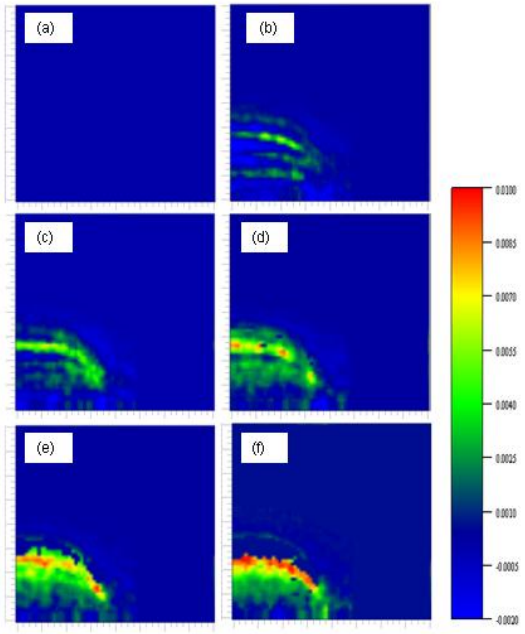

Fig.6 Color contours of the toroidal flow velocity for impurity ions. Figures are shown in the same manner as Fig. 3.

tends to coincide with the plasma velocity. At the separatrix, however, it is not necessary the case that the toroidal friction force results in the toroidal flow because of relatively strong fields.

The toroidal velocity of impurity ions measured by the Doppler shift of the spectral line is shown in Fig. 9.

The line of sight is shifted away from the geometric axis by 4.5 cm; it locates between the field-null and the separatrix. We find the toroidal velocity of the impurity ions is about $0.065 v_{A0}$ after $t = 9 t_{A0}$ from the formation of the FRC plasma. This velocity measured by the experiment sits between the field-null and separatrix flow velocity obtained by our calculation. However, a detailed comparison of the flow profile should be done in a near future. Also, we need to add the electron pressure gradient term in the electric field for a more valid estimation of the impurity flow velocity.

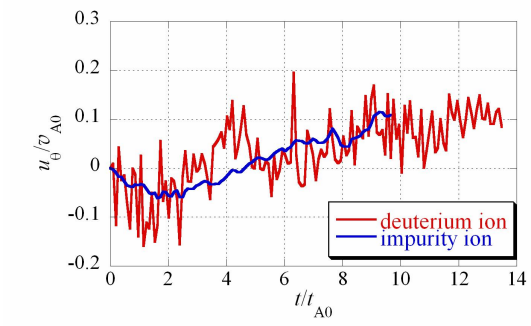

Fig.7 The time evolution of the toroidal velocity at the field-null point for the deuterium ions (the red line) and the impurity ions (the blue line).

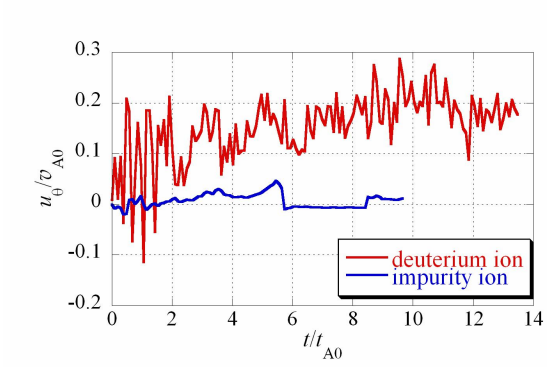

Fig.8 The time evolution of the toroidal velocity at the separatrix and midplane for the deuterium ions (the red line) and the impurity ions (the blue line).

4. Summary

We have calculated numerically orbits of the impurity ions (C^{4+}) to study the difference of the toroidal rotation velocity between impurity and plasma ions in a field-reversed configuration (FRC) plasma. The flux of the FRC plasma decays resistively, and plasma ions gradually gain the toroidal momentum. The impurity ions also spin-up at the field-null point due to the friction force from the plasma ions, and their rotation velocity gives close agreement with the flow velocity of the plasma. The separatrix flow velocity for impurity ions, however, tends to deviate from the plasma ion velocity. Because of a relatively strong field at the separatrix, the friction force between plasma and impurity ions is found to affect little their rotation velocity. Therefore, we consider modification of the Doppler shift measurement is necessary for the toroidal velocity near the separatrix.

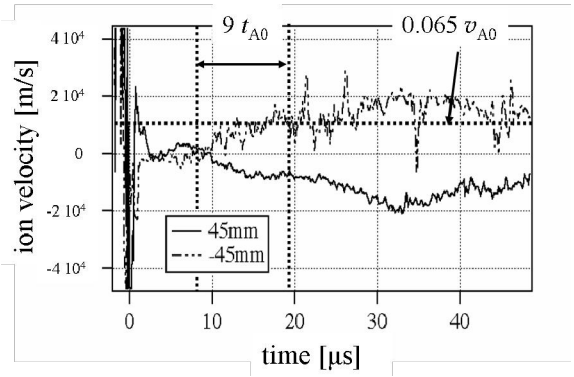

Fig.9 The time evolution of the toroidal velocity of impurity ions that is measured by the Doppler shift measurement.

References

[1] M. Tuszewski, Nucl. Fusion **28**, 2033 (1988).
[2] D. J. Rej et al., Phys. Fluids B **4**, 1909 (1992).
[3] S. Ohi *et al*. Phys. Rev. Lett. **51**, 1042 (1983).
[4] S. Shimamura and Y. Nogi, Fusion Technol. **9**, 69 (1986).
[5] T. Asai *et al*, Phys. Plasmas **13**, 072508 (2006).
[6] D. S. Harned and D. W. Hewett, Nucl. Fusion **24**, 201 (1984).
[7] L. C. Steinhauer, Phys. Plasmas **9**, 3851 (2002).
[8] E. V. Belova *et al*., Nucl. Fusion **46**, 162 (2006).
[9] T. Takahashi *et al*., Plasma Fusion Res. **2**, 002 (2007).
[10] A. H. Boozer and G. K.-Petravic, Phys. Fluids **24**, 851 (1981).
[11] C. K. Birdsall and A. B. Langdon, in *Plasma Physics via Computer Simulation* (Institute of Physics Publishing, Bristol and Philadelphia, 1991).